Journal of Organometallic Chemistry 694 (2009) 2717–2726

Contents lists available at ScienceDirect

Journal of Organometallic Chemistry

journal homepage: www.elsevier.com/locate/jorganchem

Harvesting solar energy using conjugated metallopolyyne donors containing electron-rich phenothiazine–oligothiophene moieties

Wai-Yeung Wong [a,*], Wing-Cheong Chow [a], Kai-Yin Cheung [b], Man-Kin Fung [b], Aleksandra B. Djurišić [b,*], Wai-Kin Chan [c]

[a] Department of Chemistry and Centre for Advanced Luminescence Materials, Hong Kong Baptist University, Waterloo Road, Kowloon Tong, Hong Kong, PR China
[b] Department of Physics, The University of Hong Kong, Pokfulam Road, Hong Kong, PR China
[c] Department of Chemistry, The University of Hong Kong, Pokfulam Road, Hong Kong, PR China

ARTICLE INFO

Article history:
Received 18 January 2009
Received in revised form 9 February 2009
Accepted 9 February 2009
Available online 21 February 2009

Keywords:
Metallopolyynes
Phenothiazine
Photovoltaics
Oligothiophene
Platinum

ABSTRACT

A new family of soluble, solution-processable metallopolyynes of platinum(II) functionalized with electron-rich phenothiazine–oligothiophene rings and their corresponding dinuclear model complexes were synthesized and characterized. The organometallic polymers show different degrees of absorption capabilities in the solar spectral region, rendering some of them good electron donors for fabricating bulk heterojunction polymer solar cells by blending with a methanofullerene electron acceptor. The influence of the number of thienyl rings along the polymer chain on the optical and photovoltaic properties of these metallopolymers was studied. At the same donor:acceptor blend ratio of 1:4 or 1:5, the light-harvesting capability and solar cell efficiency notably increase as the number of thienyl rings is doubled. Photoexcitation of the polymer solar cells results in a photoinduced electron transfer from the π-conjugated metallopolyyne to [6,6]-phenyl C_{61}-butyric acid methyl ester and the best-performing polymer showed a power conversion efficiency (PCE) up to ~1.3% with a corresponding peak external quantum efficiency of 63% under air mass (AM1.5) simulated solar illumination even at shorter absorption wavelength regime. The power dependencies of the solar cell parameters (including the short-circuit current density, open-circuit voltage, fill-factor and PCE) were also tested in detail.

1. Introduction

Energy and environment have been recognized as two of the top challenges of the human beings nowadays. Sunlight is perhaps the most abundant, renewable and clean energy source on the Earth. Therefore, the strong demand to harvest solar energy stimulates intensive scientific research for efficient, low-cost, lightweight photovoltaic devices [1–4]. Polymer-based organic photovoltaic systems hold the promise for a cost-effective, lightweight solar energy conversion platform as compared to the inorganic semiconductors and have potential to excel in large-area flexible devices [5–8]. Encouraging progress has been made over the past few years in the area of bulk heterojunction polymer solar cells (PSCs) based on polymer donors and molecular acceptors in blends [9] but many issues of materials and device development remain yet to be addressed. To date, poly(3-hexylthiophene):[6,6]-phenyl-C_{61}-butyric acid methyl ester (P3HT:PCBM) represents a promising active layer material in PSCs with power conversion efficiencies (PCEs) approaching 5–6% [10–19]. The current state-of-the-art in this growing field is critically examined with a focus on improving or optimizing the electronic and morphological interactions of the polymer and the fullerene.

Recently, conjugated organic polymers containing metal centers in the main chain have evolved as a new class of active materials to capture energy from the Sun [20–37] and this interest derives from the fact that incorporation of heavy metals into an organic conjugated framework can elicit huge effects on the electronic and optical properties of the polymers [38–47]. Among these, metallopolyynes stand out to be particularly interesting candidates in this area [23–36]. For a rational design of solar cells with the aim of optimizing solar spectrum coverage and charge mobility, both in single and tandem cells, it is very desirable to seek for a new class of conjugated polymers with tunable functional properties for PSCs so that they can be processed under similar conditions and the cell design and optimization processes can be simplified [48–55]. It has been shown that organic groups such as fluorene [35], 2,1,3-benzothiadiazole [31,34], thieno[3,4-b]pyrazine [36] and bithiazole [32] can be used to prepare efficient organometallic PSCs with the photosensitivity at longer wavelengths due to their narrow bandgaps. In each of these cases, inclusion of various thiophene fragments into the (hetero)arylene unit is likely to further expand the spectral

* Corresponding authors. Tel.: 852 34117074; fax: 852 34117348 (W.-Y. Wong).
E-mail addresses: rwywong@hkbu.edu.hk (W.-Y. Wong), dalek@hkusua.hku.hk (A.B. Djurišić).

0022-328X/$ - see front matter © 2009 Elsevier B.V. All rights reserved.
doi:10.1016/j.jorganchem.2009.02.006

width of absorption appropriate for sunlight harvesting. Following this line, we report here the synthesis, characterization and photovoltaic behavior of some bandgap-tunable metallopolyynes containing the bis(oligothienyl)-phenothiazine spacer. Phenothiazine (PTZ) belongs to an important class of tricyclic nitrogen–sulfur heterocycles [56], with a broad spectrum of pharmacological activity [57–63] Phenothiazine has low and highly reversible first oxidation potentials [64–67] with pronounced propensities to form stable radical cations. Also, phenothiazine and its derivatives serve as good intramolecular reductive quenchers because they show a facile one electron oxidation, and the PTZ radical cation ($PTZ^{\cdot+}$) is known to have a strong absorption in the visible region [68–69] This makes the identification of the charge-separated intermediate formed upon electron transfer from PTZ to the ^{3}MLCT excited state of the chromophore unambiguous [70–73]. The electron-rich nature of phenothiazine makes it a good electron donor in some studies related to donor-chromophore–acceptor triad for photoinduced charge separation [70–73] and it is also a good electron donor for reductive quenching [74,75]. As a consequence, these favorable electronic properties of phenothiazines have led to their application as electrophore probes in supramolecular assemblies for photoinduced electron transfer (PET) studies and as electron donor components in various optical and electronic domains [76–79] The prospect of integrating strongly coupled redox-active phenothiazine fragment into conjugated oligothiophene chains could constitute a new class of spacers in optoelectronically-active metallopolyynes. In our studies, PSCs derived from them showed PCEs of up to 1.3% even at shorter visible wavelengths. The work permits a chemical tuning of the PCE by modulating the number of thienyl rings in the organic chromophore, which changes the absorption features and possibly charge transport properties of the resulting polymers.

2. Results and discussion

2.1. Synthetic methodologies and chemical characterization

The chemical structures of new platinum(II) polyyne polymers **P0**–**P2** and their selected well-defined model compounds **M0**–**M2** are shown in Scheme 1. The dibromo precursors (**L1–2Br** and **L2–2Br**) can be obtained from **L0–2Br** by successive coupling of 2-thienylmagnesium bromide with the corresponding phenothiazine-based dibromide of the lower generation. Conversion of the dibromide derivatives to their corresponding diethynyl congeners can be readily achieved following the typical organic synthetic protocols for alkynylation of aromatic halides [70,80]. It is worth noting that the purification steps become more tedious in the ligand synthesis as the number of thienyl rings m increases. The Pt alkynyl compounds were prepared by the Sonogashira-type dehydrohalogenation between each of the diethynyl precursors and suitable platinum chloro precursors [23–36,81–90]. The feed mole ratio of the platinum precursors and the diethynyl ligands were 1:1 and 2:1 for the polymer and dimer syntheses, respectively, and each product was carefully purified to remove ionic impurities and catalyst residues. The use of a long dodecahexyl chain on phenothiazine is crucial in increasing the solubility and improving the solution processability/tractability of these metallopolyynes. The dinuclear Pt complexes serve as good discrete molecular model complexes for the corresponding polymers as far as their spectroscopic and photophysical properties are concerned. The polymers can be purified by silica column chromatography and repeated precipitation and isolated in good yield and high purity. Yields of the polymers are between 57% and 60%. All of these Pt compounds are thermally and air-stable solids and they are soluble in common chlorinated hydrocarbons and toluene. However, it appears that the non-thiophene species **L0**, **M0** and **P0** are not very stable in solution under ambient conditions or on exposure to light for long periods and so they should be freshly prepared for subsequent characterization. **P0**–**P2** can cast tough, free-standing thin films from their solutions readily but their solubility tends to decrease gradually as m increases. Gel-permeation chromatography (GPC) on **P0**–**P2** suggests their oligomeric/polymeric nature. The relatively narrow polydispersity (PDI $\sim$ 1.68–2.01) in molecular weights is consistent with the proposed linear structure from the condensation polymerization. The number-average molecular weights (M_n) of **P0**–**P2** calibrated with polystyrene standards range from 11 350 to 16 070 and **P1** and **P2** can possess up to $\sim$21–25 heterocyclic rings in total along the polymer chain based on M_n. Since a certain portion of **P2** formed (m = 2) was organic insoluble, the molecular weight of the soluble fraction is believed to be relatively low. The structures were unequivocally characterized using elemental analyses, mass spectrometry, IR and NMR spectroscopies (see Section 4).

2.2. Photophysical and electrochemical characterization

The absorption and emission spectra of the polymers and model complexes were measured in CH_2Cl_2 solutions at 293 K (see Table 1 and Figs. 1 and 2 for **P0**–**P2**). The absorption of **P0**–**P2** is each dominated by an intense ligand-centered π–π^* transitions in the oligothienyl-phenothiazine organic system peaking at 349–430 nm, and these polymers emit strong fluorescence from the singlet excited states at 465–533 nm under ambient conditions. The absorption and emission properties of the diplatinum model compounds **M0**–**M2** are very similar to those of their polymeric congeners (see Supplementary material (SM)). The featureless absorption pattern is typical of many π-conjugated polymers and arises in part from the distribution of the conjugation lengths. Due to the presence of an extended π-electron delocalized system through the rigid phenothiazine–oligothiophene segment and the electron-rich Pt ion, the bandgaps of **P0**–**P2** vary from 2.90 to 2.52 eV with the value for orange-red **P2** significantly lowered by ca. 0.38 eV relative to the yellow-brown neat phenothiazine-based **P0**. However, the extent of bathochromic shifts induced by increasing m is less pronounced and there would be little advantage in extending the π-conjugation length by increasing m too much given the increased synthetic and purification complication and much reduced product yields. A linear oligothienyl chain length dependence of E_g can be rationalized from the plot of E_g against reciprocal chain length ($1/a$, where $a = m + 1$) and a limiting value for E_g is estimated to be ca. 2.34 eV for $m = \infty$ (Fig. 3) [91–93]. The measured photoluminescence (PL) lifetimes for **P0**–**P2** and **M0**–**M2** for the main peaks are all very short (ca. 1.23–1.81 ns) at 293 K, characteristic of the spin-allowed singlet emission. These results together with the small Stokes shift observed preclude the emitting state as a triplet excited state [23]. While a strong triplet emission at 551 (543) nm, with a substantially larger Stokes shift and a triplet emissive lifetime τ_P of ca. 2.09 (2.15) μs, is detectable in the PL spectrum of **P0** (**M0**) at 77 K (Figs. 4 and 5), we observed no such long-lived emission over the measured spectral window between 1.2 and 3.1 eV for **P1**–**P2**. The phosphorescence to fluorescence intensity ratio is higher for **P0** than that for **M0** at 77 K. The observation of efficient triplet emission is intrinsically more difficult for low-bandgap polyynes such as **P1**–**P2**, which manifests the fate of energy gap law for Pt-containing conjugated polyynes and their model diynes [94]. Theoretically, the law predicts that the rate of radiationless deactivation increases as the emission gap decreases due to the matching of wavefunctions between the emitting state and highly vibrational levels of the ground electronic state, resulting in a fast $T_1 \rightarrow S_0$ internal conversion, followed by the solvent (or lattice in the solid state) deactivation. This quenching mechanism is intrinsic and probably poses the main obstacle for phosphorescence for **P1**–**P2**. In addition, the fully

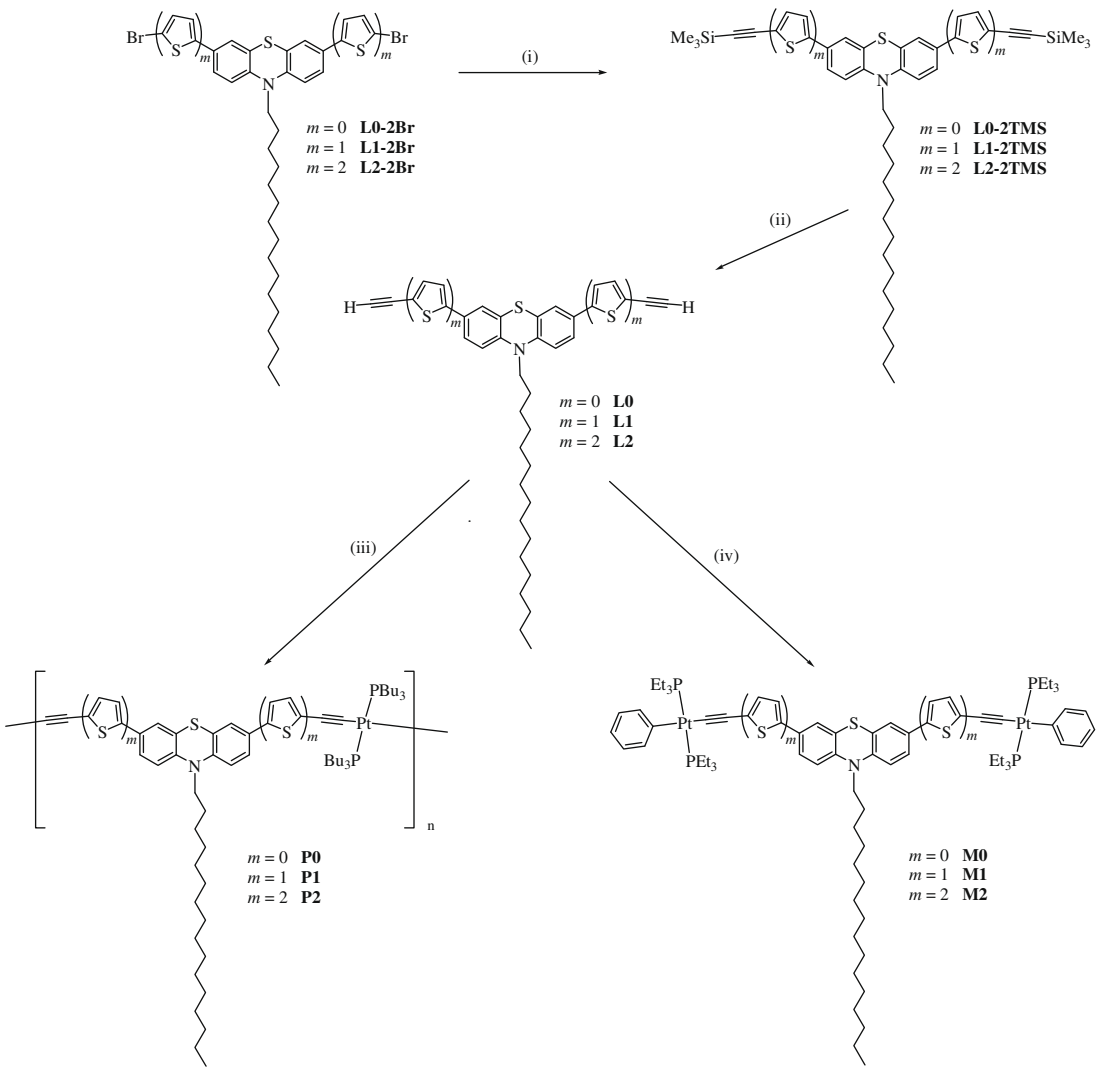

Reagents and conditions: (i) $Me_3SiC{\equiv}CH$, CuI, $Pd(OAc)_2$, PPh_3, NEt_3; (ii) K_2CO_3, MeOH; (iii) *trans*-$[PtCl_2(PBu_3)_2]$, CuI, NEt_3; (iv) *trans*-$[PtPh(Cl)(PEt_3)_2]$, CuI, NEt_3

Scheme 1. Synthesis of phenothiazine-based diethynyl ligands and their Pt(II) complexes.

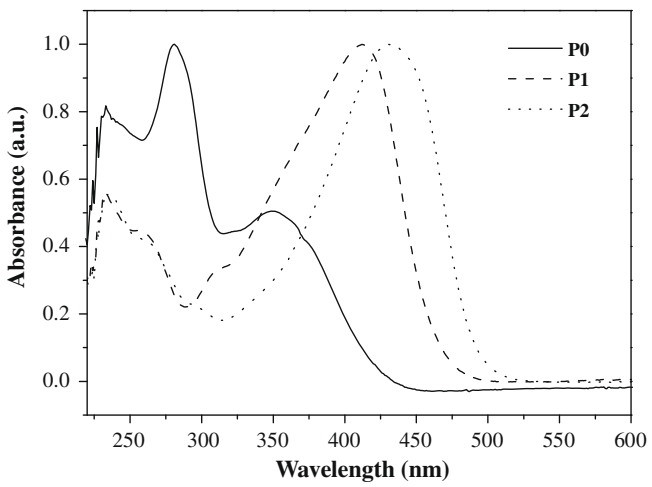

Fig. 1. Absorption spectra of **P0**–**P2** in CH_2Cl_2 solution at 293 K.

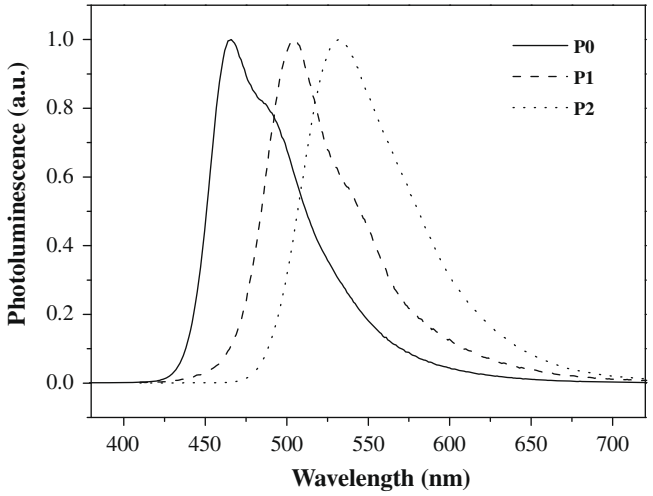

Fig. 2. PL spectra of **P0**–**P2** in CH_2Cl_2 solution at 293 K.

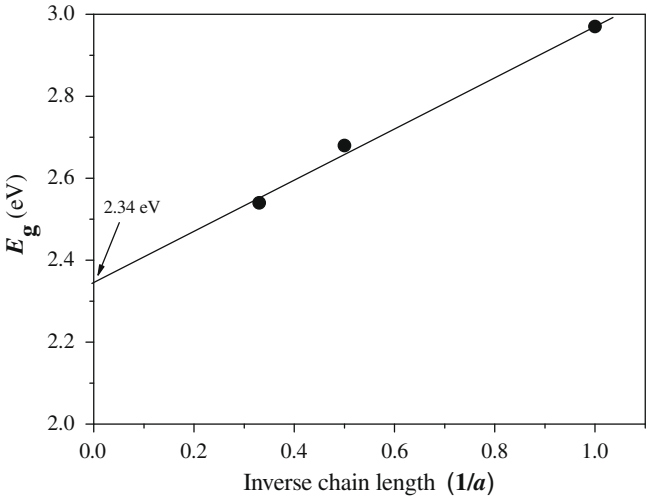

Fig. 3. Relationship of E_g and $1/a$ ($a = m + 1$) for **P0**–**P2**.

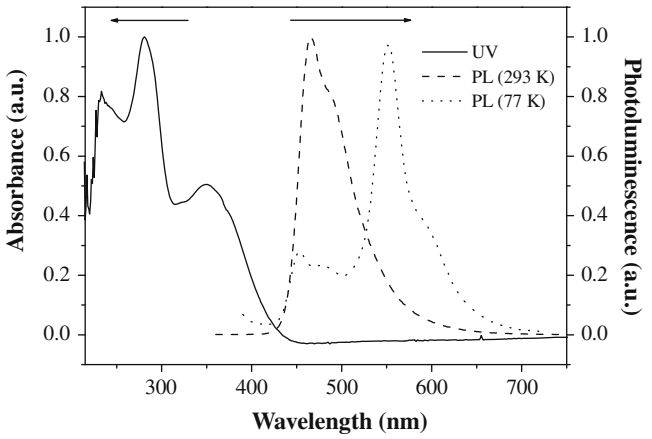

Fig. 4. Absorption (293 K) and PL (both 293 and 77 K) spectra of **P0** in CH_2Cl_2 solution.

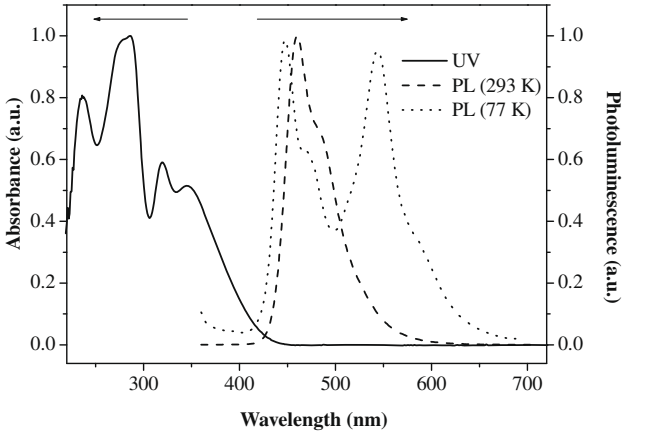

Fig. 5. Absorption (293 K) and PL (both 293 and 77 K) spectra of **M0** in CH_2Cl_2 solution.

extended heteroaryl rings in the ligand chromophore greatly reduces the influence of heavy metal ion in **P1**–**P2** which is mainly responsible for the intersystem crossing and hence the phosphorescence. Therefore, we consider a ligand-dominating singlet excited state instead of the triplet state to contribute to the efficient photo-induced charge separation in the energy conversion for **P1**–**P2**, which contrasts with the Pt-monothiophene polyyne-based blends where charge separation takes place via the triplet state channel of the polymer [23]. From the solvent dependence studies of the emission spectra of **P1**–**P2**, it is also unlikely to ascribe the localized states centered at 2.30–2.50 eV to a strong charge-transfer-type interaction for **P1**–**P2** since there is no evidence of strong solvatochromism in solvents of various polarities (see SM). Presumably, this is the case because the present system does not consist of alternating donor–π-acceptor structural units along the polymer chain. Since the PL efficiency generally reduces as the size of a molecule is increased as a result of a greater number of quenching sites and the possibility of bimolecular decay, we note an increase in the quantum yield when going from the polymer **P0**–**P2** to its corresponding dimer **M0**–**M2**.

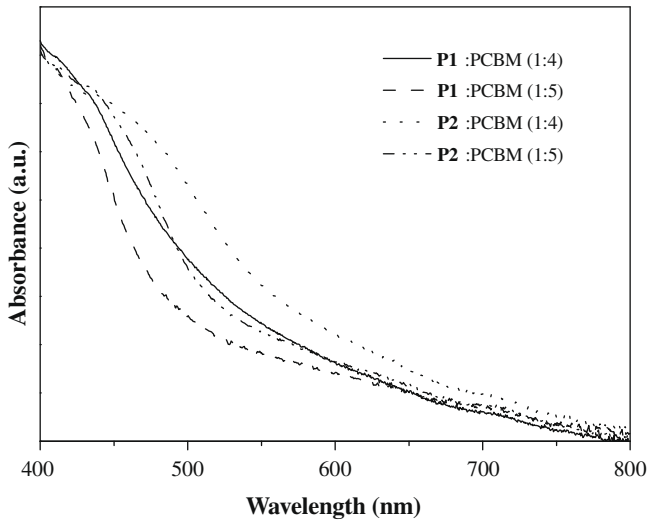

Fig. 6. Absorption spectra of polymer:PCBM blends (1:4 and 1:5, w/w).

Absorption spectra of neat **P1** and **P2** together with those blended with PCBM (1:4 and 1:5 by weight) are shown in Fig. 6 and SM. Each of the neat spectra shows one major band ($\lambda_{max} \sim 419$ and 443 nm, respectively). The higher energy peak in the blend film is less pronounced because of the dramatically enhanced absorption in the UV region by the addition of 80% or 83% PCBM.

The thermal properties of the polymers were also examined by thermal gravimetric analysis (TGA) under nitrogen (Table 1). All of them exhibited good thermal stability with the decomposition onsets at ~345–366 °C, which are higher than those for *trans*-$[Pt(PBu_3)_2C{\equiv}CArC{\equiv}C]_n$ (Ar = C_6H_4, 300 °C [30,83], anthrylene, 315 °C [95], oligothienylene, 278–290 °C [26], etc.). Decomposition onset was defined by a 5 wt.% loss in each case.

The highest occupied molecular orbital (HOMO) and the lowest unoccupied molecular orbital (LUMO) levels of stable Pt polyynes **P1**–**P2** were calculated using the redox potentials determined from electrochemical measurements using cyclic voltammetry. The experiments were performed by casting the polymer films on the glassy-carbon working electrode with a Ag/AgCl wire as the reference electrode, at a scan rate of 50 mV s^{-1}. The solvent in all measurements was deoxygenated MeCN, and the supporting electrolyte was 0.1 M $[^nBu_4N]BF_4$. The relevant data are collected in Table 2. From the onset values of oxidation potential ($E_{onset,\ ox}$) and reduction potential ($E_{onset,\ red}$), the HOMO and LUMO levels of the polymers were calculated according to the following equations $E_{HOMO} = -(E_{onset,\ ox} + 4.72)$ eV and $E_{LUMO} = -(E_{onset,\ red} + 4.72)$ eV (where the unit of potential is V versus Ag/AgCl) [96–97] From some literature data, the phenothiazine ring mainly influences

Table 1
Photophysical and thermal data of **P0**–**P2** and **M0**–**M2**.

	Absorption (293 K)		Emission (293 K)			Emission (77 K)		T_{dec} (°C)
	λ_{abs} (nm) CH_2Cl_2[a]	Bandgap E_g (eV)[b]	λ_{em} (nm) CH_2Cl_2	Φ (%)	τ_P (ns)	λ_{em} (nm) CH_2Cl_2	τ_P (ns)	
P0	281, 349	2.90	465, 491*	5.4	1.49	452*, 480*, 551, 593*	2.09×10^3	348
P1	262, 314, 412	2.66	505, 537*	1.6	1.38	494, 540*	1.67	345
P2	264, 430	2.52	533	4.1	1.23	537, 572*	1.59	366
M0	286 (4.0), 320 (1.8), 346 (1.4)	2.93	460, 485*	10.3	1.45	447, 470*, 543	2.15×10^3	
M1	257 (2.0), 312 (0.1), 355 (4.7), 402 (4.5)	2.68	502, 533*	5.3	1.65	491, 525*	2.04	
M2	263* (3.4), 300* (1.6), 426 (6.4)	2.54	527	7.8	1.81	524, 561*	1.87	

Asterisks indicate weak or shoulder bands.
[a] Molar extinction coefficients (10^4 dm^3 mol^{-1} cm^{-1}) are shown in parentheses.
[b] Optical bandgaps determined from the onset of absorption in solution phases.

Table 2
Electrochemical data and frontier orbital energy levels for **P1** and **P2**.

Polymer	Oxidation potential (V)	Energy levels (eV)		Bandgap (eV)
	$E_{onset,\ ox}$[a]	E_{HOMO}[b]	E_{LUMO}[c]	E_g^{opt}[d]
P1	+0.84	−5.56	−2.87	2.66
P2	+0.79	−5.51	−3.00	2.52

[a] $E_{onset,\ ox}$ are the onset potentials of oxidation.
[b] $E_{HOMO} = -(E_{onset,\ ox} + 4.72)$ eV.
[c] Calculated from the optical bandgap and the energy level of HOMO and $E_{LUMO} = (E_{HOMO} + E_g^{opt})$ eV.
[d] E_g^{opt} = Optical bandgap.

the oxidation (*p*-doping) process of the polymer [66,67,70]. Each of **P1**–**P2** shows a quasi-reversible phenothiazinyl oxidation at 0.84 and 0.79 V, respectively, and the oxidation potential is reduced with increasing thienyl chain length *m*, consistent with the phenomenon that delocalization of the generated phenothiazine radical cations is apparently more favored and stabilized by increased conjugation length [98–105] For **P2**, two additional anodic waves due to the bithienyl cores also appeared at the more positive potentials peaking at ca. 1.06 and 1.32 V but it was shown to be absent for **P1**. The electrooxidation of oligothiophenes is often irreversible because the electrogenerated cations readily undergo rapid coupling reactions leading to higher oligomers or polymers. Hence, the HOMO levels tend to be elevated with increasing *m* from **P1** (−5.56 eV) to **P2** (−5.51 eV). However, no reduction wave was observed in both cases.

2.3. Polymer solar cell behavior

Polymer solar cells were fabricated by using each of **P1**–**P2** as an electron donor and PCBM as an electron acceptor (Table 3). The hole collection electrode consisted of indium tin oxide (ITO) with a spin-coated poly(3,4-ethylene-dioxythiophene):poly(styrene sulfonate) (PEDOT:PSS), while Al served as the electron collecting electrode. We consider that enhancing the absorption coefficient of the band by increasing the conjugation chain length with oligothienyl rings is an effective way to improve the cell performance. The versatile functionalization of thiophene groups on phenothiazine also allows a good synthetic means of tuning the solubility, polarity and bandgap in metallopolyynes. A marked increase in the short-circuit current density (J_{sc}) and PCE can be observed in **P2** relative to **P1** at the same blend ratio (Fig. 7a). It is remarkable to see that the light-harvesting ability of **P2** (with its commensurately better light absorption characteristics than **P1**) can be increased by over 0.2–0.3% relative to **P1** simply by adding two more thienyl rings along the main chain. This is in agreement with the increased absorption coefficients with increasing *m* from **M1** to **M2** (see Table 1), resulting in higher PCE for **P2**. With reference to some recent studies in related systems [32,35], it is possible that for both electrons and holes, the mobilities increase with increasing *m* in **P1**–**P2**. A PCE of up to 1.06–1.29% can be obtained for **P1** and **P2** ($E_g \sim 2.66$ and 2.52 eV, respectively) at the same blend ratio of 1:5 under illumination of an AM1.5 solar simulator. The shape of the external quantum efficiency (EQE) curve follows the shape of the absorption of the blend and **P2** has a slightly higher absorption at longer wavelengths. The EQE curves for **P1** and **P2** show a maximum of 64.2 (for 1:5 blend ratio) and 68.9% (for 1:4 blend ratio), respectively (Fig. 7b). Preliminary AFM images of the 1:4 and 1:5 blends for both **P1** and **P2** show that the films are rather smooth and do not show large domain sizes (see SM). Both the V_{oc} and FF values of **P1**- and **P2**-based solar cells (1:5) are quite close to each other. The fill-factor (FF) ranges from 0.30 to 0.41 for the best devices. The relatively low values are at least partly due to the fact that all processing (except PEDOT:PSS annealing and electrode deposition) and measurements have been done in ambient atmosphere which likely results in the presence of traps. We expect FF to improve for fabrication and characterization to be performed in inert gas environment. Comprehensive study of charge transport and the influence of traps is necessary to further improve FF and overall device performance.

To study the performance of PSCs, it is vital to understand which mechanisms control the *J*–*V* characteristics of a given device and the fate of the photogenerated electrons and holes. So, the influence of light intensity on the solar cell parameters is very informative for analyzing internal recombination losses [106,107]. The *J*–*V* curves for **P2** under different excitation powers and the power dependence of the solar cell parameters are shown in Figs. 8 and 9, respectively. The J_{SC} exhibits a linear dependence

Table 3
Solar cell performance of best devices with **P1** and **P2**. The numbers in parentheses denote average from 6 devices. For EQE maxima, the numbers in brackets denote the wavelength in nm at which maximum occurs.

PSC	V_{oc} (V)	J_{sc} (mA cm^{-2})	FF	Max. PCE (%)	Max. EQE (%)
P1:PCBM (1:4)	0.63 (0.61)	2.73 (2.60)	0.32 (0.31)	0.55 (0.50)	57.6 (409)
P1:PCBM (1:5)	0.78 (0.76)	3.71 (3.70)	0.37 (0.37)	1.06 (1.03)	64.2 (415)
P2:PCBM (1:4)	0.73 (0.73)	3.95 (3.80)	0.30 (0.29)	0.86 (0.80)	68.9 (415)
P2:PCBM (1:5)	0.79 (0.78)	4.06 (4.00)	0.41 (0.39)	1.29 (1.27)	63.2 (415)

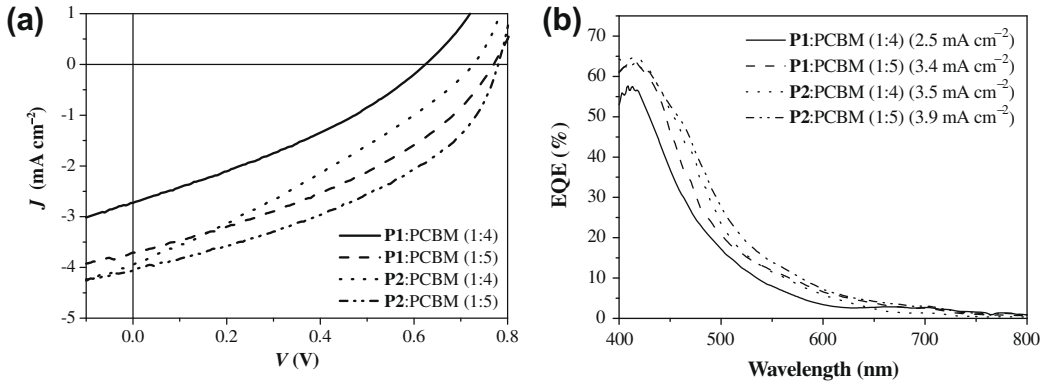

Fig. 7. (a) J–V curves of solar cells with **P1**–**P2**:PCBM (1:4 and 1:5, w/w) active layers under simulated AM1.5 solar irradiation. (b) EQE wavelength dependencies of solar cells with **P1**–**P2**:PCBM (1:4 and 1:5, w/w) active layers. Current density estimates in brackets were calculated by integration, for a given EQE curve and assuming ideal AM 1.5 spectrum.

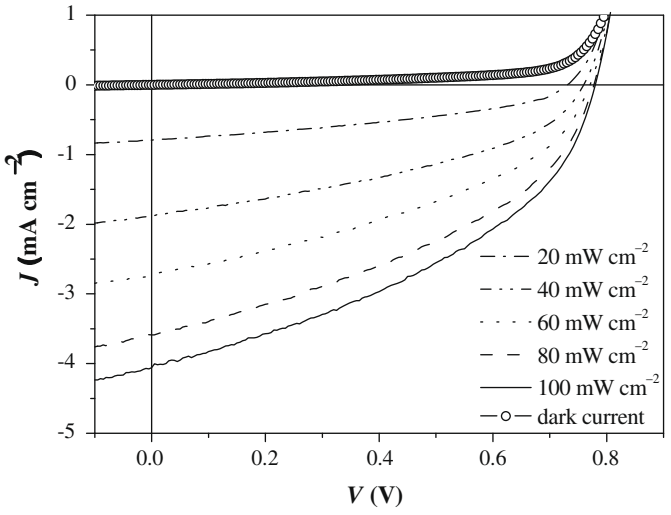

Fig. 8. J–V curves of the **P2**:PCBM (1:5) device for different illumination.

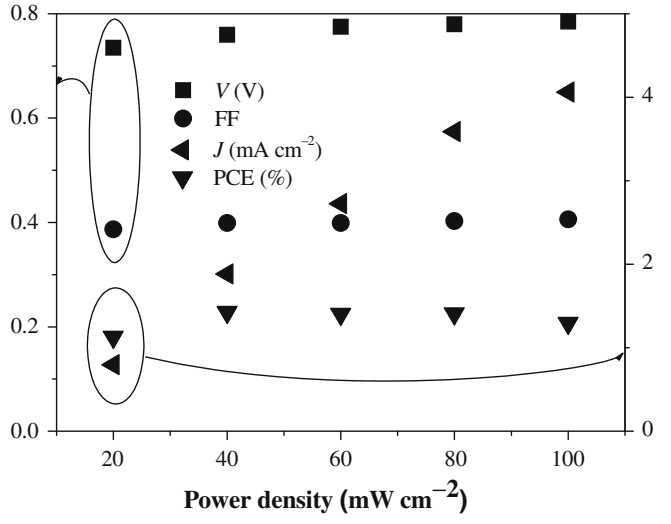

Fig. 9. Power dependencies of open-circuit voltage (V_{OC}), short-circuit current density (J_{SC}), fill-factor (FF) and power conversion efficiency (PCE) for the **P2**:PCBM (1:5) cells.

on the optical power, while V_{oc} shows some increase and then saturates at higher intensity, which is expected [108]. The PCE only decreases slightly with the illumination intensity, reaching a peak of 1.43% at 40 mW cm^{-2}. The FF shows a maximum of 0.41 at the benchmark power level of 100 mW cm^{-2}.

3. Conclusion

In summary, we have established a versatile system for preparing phenothiazine-based conjugated platinum(II) metallopolyynes with tunable optical absorption, electrochemical and electronic properties for PSCs by suitable manipulation of the oligothienyl chain length. This in turn can improve the performance of the resulting PSCs through extending the oligothienyl chain length in polyplatinynes, and we have attained PCE as high as 1.3% under simulated AM1.5 solar illumination even for photosensitivity at shorter wavelengths. Polymers **P1** and **P2** represent new examples of high-bandgap organometallic polymers ($E_g > 2.5$ eV) with a strongly blue-absorbing chromophore for harvesting solar radiation. Given the performance and processing advantages, this work has great potential to excel for the realization of more practical devices even without the need for exploiting the triplet excited states in promoting an efficient photoinduced charge separation. It clearly sets out a rarely explored strategy toward an effective tuning of the solar cell efficiency and charge transport properties in conjugated metallopolymers for the next stage of development for reliable polymer-based solar power generation. It is expected that optimization at all levels of device construction and blend composition will result in further improvements in the efficiency. Also, the dependence of solar cell performance on molecular weight should not be overlooked, which can cause significant changes in the blend morphology, and such a study is currently under active investigation in our laboratories.

4. Experimental

4.1. General information

Solvents were carefully dried and distilled from appropriate drying agents prior to use. Commercially available reagents were used without further purification unless otherwise stated. All reagents for the chemical syntheses were purchased from Aldrich or Acros Organics. PCBM and regioregular P3HT (weight-average molecular weight M_w 20000–50000) were purchased from American Dyes. PEDOT:PSS (Baytron VPAI 4083) was purchased from

H.C. Starck. Reactions and manipulations were carried out under an atmosphere of prepurified nitrogen using Schlenk techniques. All reactions were monitored by thin-layer chromatography (TLC) with Merck pre-coated glass plates. Flash column chromatography and preparative TLC were carried out using silica gel from Merck (230–400 mesh). Infrared spectra were recorded as CH_2Cl_2 solutions using a Perkin–Elmer Paragon 1000 PC or Nicolet Magna 550 Series II FTIR spectrometer, using CaF_2 cells with a 0.5 mm path length. Fast atom bombardment (FAB) mass spectra were recorded on a Finnigan MAT SSQ710 system. NMR spectra were measured in $CDCl_3$ on a Varian Inova 400 MHz FT-NMR spectrometer and chemical shifts are quoted relative to tetramethylsilane for ^1H and ^{13}C nuclei and H_3PO_4 for ^{31}P nucleus.

4.2. Physical measurements

UV–Vis spectra were obtained on an HP-8453 diode array spectrophotometer. The solution emission spectra and lifetimes of the compounds were measured on a Photon Technology International (PTI) Fluorescence QuantaMaster Series QM1 spectrophotometer. The phosphorescence quantum yields were determined in degassed CH_2Cl_2 solutions at 293 K against quinine sulfate in 0.1 N H_2SO_4 ($\Phi_F = 0.54$) [109]. The decay curves were analyzed using a Marquardt-based nonlinear least-squares fitting routine and were shown to follow a single-exponential function in each case according to $I = I_0 + A\exp(-t/\tau)$. The CV measurements were carried out at a scan rate of 50 mV s^{-1} using a eDAQ EA161 potentiostat electrochemical interface equipped with a thin film coated ITO covered glass working electrode, a platinum counter electrode and a Ag/AgCl (in 3 M KCl) reference electrode. The solvent in all measurements was deoxygenated MeCN, and the supporting electrolyte was 0.1 M [$^nBu_4N$]BF_4. Thin polymer films were deposited on the working electrode by dip-coating in chlorobenzene solution (6 mg mL^{-1}). The onset oxidation and reduction potentials were used to determine the HOMO and LUMO energy levels using the equations $E_{HOMO} = [-(E_{onset,\ ox\ (vs.\ Ag/AgCl)} - E_{onset\ (N.H.E.\ vs.\ Ag/AgCl)}] - 4.50$ eV and $E_{LUMO} = [-(E_{onset,\ red\ (vs.\ Ag/AgCl)} - E_{onset\ (N.H.E.\ vs.\ Ag/AgCl)}] - 4.50$ eV, where the potentials for N.H.E. versus vacuum and N.H.E. versus Ag/AgCl are 4.50 and −0.22 V, respectively [96,97].

4.3. Preparation of compounds

4.3.1. Synthesis of *L0-2TMS*

L0-2Br (2.00 g, 3.44 mmol), CuI (50 mg), $Pd(OAc)_2$ (50 mg) and PPh_3 (150 mg) were combined in NEt_3 (60 mL) and THF (100 mL) to yield a yellow solution. $Me_3SiC{\equiv}CH$ (0.97 mL, 6.88 mmol) was added dropwise to the reaction mixture at room temperature and the mixture was stirred for 2 h. The mixture was then heated up to 70 °C for 15 h to give a deep brown solution mixture. The completion of the reaction was verified by spot TLC. The solvent was evaporated to dryness. The residue was redissolved in CH_2Cl_2 and subjected to purification by column chromatography using CH_2Cl_2/*n*-hexane (1:3, v/v) as eluent to afford a yellow solid of **L0-2TMS** (1.46 g, 69%).

Spectral data: IR (KBr): 2155 cm^{-1} (C≡C). ^1H NMR ($CDCl_3$): δ = 7.24 (m, 2H, Ar), 7.19 (m, 2H, Ar), 6.69 (d, J = 8.0 Hz, 2H, Ar), 3.75 (t, J = 8.0 Hz, 2H, $NCH_2(CH_2)_{14}CH_3$), 1.75–1.70 (m, 2H, $NCH_2CH_2(CH_2)_{13}CH_3$), 1.39–1.28 (m, 26H, $NCH_2CH_2(CH_2)_{13}CH_3$), 0.93 (t, J = 8.0 Hz, 3H, $NCH_2CH_2(CH_2)_{13}CH_3$), 0.29 ppm (s, 18H, $Si(CH_3)_3$). ^{13}C NMR ($CDCl_3$): δ = 145.27, 131.79, 131.14, 124.60, 117.90, 115.68, 115.57 (Ar), 105.04, 94.58 (C≡C) 54.01, 48.18, 32.61, 30.38, 30.34, 30.29, 30.17, 30.05, 29.80, 27.34, 27.22, 23.37, 14.82 ($C_{16}H_{33}$) 0.69 ppm ($Si(CH_3)_3$). FAB-MS: m/z = 616 (M^+). Anal. Calc. for $C_{38}H_{57}NSSi_2$: C, 74.08; H, 9.33; N, 2.27. Found: C, 73.92; H, 9.10; N, 2.21%.

4.3.2. Synthesis of *L1-2TMS* and *L2-2TMS*

They were prepared following the same procedures as for **L0-2TMS** but **L1–2Br** or **L2–2Br** was used instead.

L1-2TMS: Yellow solid (65%). *Spectral data*: IR (KBr): 2146 cm^{-1} (C≡C). ^1H NMR ($CDCl_3$): δ = 7.28 (m, 4H, Ar), 7.17 (m, 2H, Ar), 7.01 (m, 2H, Ar), 6.74 (d, J = 8.0 Hz, 2H, Ar), 3.76 (m, 2H, $NCH_2(CH_2)_{14}CH_3$), 1.76 (m, 2H, $NCH_2CH_2(CH_2)_{13}CH_3$), 1.40–1.26 (m, 26H, $NCH_2CH_2(CH_2)_{13}CH_3$), 0.91 (t, J = 8.0 Hz, 6H, $NCH_2CH_2(CH_2)_{13}CH_3$), 0.29 ppm (s, 18H, $Si(CH_3)_3$). ^{13}C NMR ($CDCl_3$): δ = 145.06, 144.53, 134.01, 128.54, 125.20, 124.78, 124.68, 122.18, 121.82, 115.66 (Ar), 99.77, 98.12 (C≡C) 53.65, 47.85, 32.22, 29.99, 29.91, 29.81, 29.65, 29.47, 28.14, 27.10, 26.95, 26.05, 22.98, 22.41, 22.32, 14.43 ($C_{16}H_{33}$), 0.19 ppm ($Si(CH_3)_3$). FAB-MS: m/z = 780 (M^+). Anal. Calc. for $C_{46}H_{61}NS_3Si_2$: C, 70.80; H, 7.88; N, 1.79. Found: C, 70.68; H, 7.92; N, 1.92%.

L2-2TMS: Deep yellow solid (62%). *Spectral data*: IR (KBr): 2140 cm^{-1} (C≡C). ^1H NMR ($CDCl_3$): δ = 7.70–7.64 (m, 2H, Ar), 7.54 (m, 2H, Ar), 7.47 (m, 2H, Ar), 7.33–7.30 (m, 2H, Ar), 7.13–7.09 (m, 2H, Ar), 7.00 (m, 2H, Ar), 6.82 (m, 2H, Ar), 3.85–3.82 (m, 2H, $NCH_2(CH_2)_{14}CH_3$), 1.83–1.77 (m, 2H, $NCH_2CH_2(CH_2)_{13}CH_3$), 1.29–1.24 (m, 26H, $NCH_2CH_2(CH_2)_{13}CH_3$), 0.87 (t, J = 8.0 Hz, 3H, $NCH_2CH_2(CH_2)_{13}CH_3$), 0.26 ppm (s, 18H, $Si(CH_3)_3$). ^{13}C NMR ($CDCl_3$): δ = 144.45, 143.09, 139.16, 135.43, 134.06, 133.87, 133.77, 132.38, 128.67, 128.07, 125.37, 124.55, 123.71, 123.18, 121.81, 115.70 (Ar), 100.33, 97.69 (C≡C) 53.85, 47.88, 32.16, 29.94, 29.86, 29.75, 29.60, 29.43, 27.08, 26.97, 22.92, 14.36 ($C_{16}H_{33}$), 0.08 ppm ($Si(CH_3)_3$). FAB-MS: m/z = 944 (M^+). Anal. Calc. for $C_{54}H_{65}NS_5Si_2$: C, 68.66; H, 6.94; N, 1.48. Found: C, 68.53; H, 6.87; N, 1.55%.

4.3.3. Synthesis of *L0–L2*

The diethynyl ligands were prepared by the desilylation of each of TMS derivatives. A typical procedure was given for **L0** starting from **L0-2TMS**.

A mixture of **L0-2TMS** (0.80 g, 1.30 mmol) and K_2CO_3 (0.36 g, 2.60 mmol) in MeOH (30 mL) and THF (50 mL) was stirred at room temperature under nitrogen for 4 h. The solution turned deep yellow in color after the reaction. Solvent was removed under reduced pressure to leave a yellow residue. The residue was dissolved in a minimum amount of CH_2Cl_2 and was subjected to column chromatography using CH_2Cl_2/*n*-hexane (1:1, v/v) as the solvent system to afford a yellow solid characterized as **L0** (0.46 g, 75%).

Spectral data: IR (KBr): 2107 cm^{-1} (C≡C), 3303 cm^{-1} (C≡CH). ^1H NMR ($CDCl_3$): δ = 7.31–7.28 (m, 2H, Ar), 7.24 (m, 2H, Ar), 6.76 (d, J = 8.0 Hz, 2H, Ar), 3.81 (t, J = 8.0 Hz, 2H, $NCH_2CH_2(CH_2)_{13}CH_3$), 3.10 (s, 2H, C≡CH), 1.81–1.77 (m, 2H, $NCH_2CH_2(CH_2)_{13}CH_3$), 1.45–1.30 (m, 26H, $NCH_2CH_2(CH_2)_{13}CH_3$), 0.94 ppm (t, J = 8.0 Hz, 3H, $NCH_2(CH_2)_{14}CH_3$). ^{13}C NMR ($CDCl_3$): δ = 144.75, 131.22, 130.50, 123.84, 116.07, 114.86 (Ar), 82.72 (C≡C), 47.43, 31.78, 29.56, 29.52, 29.46, 29.35, 29.23, 28.99, 26.59, 26.43, 22.54, 13.99 ppm ($C_{16}H_{33}$). FAB-MS: m/z = 471 (M^+). Anal. Calc. for $C_{32}H_{41}NS$: C, 81.47; H, 8.76; N, 2.97. Found: C, 81.56; H, 8.65; N, 2.89%.

L1: Yellow solid (68%). *Spectral data*: IR (KBr): 2103 cm^{-1} (C≡C), 3300 cm^{-1} (C≡CH). ^1H NMR ($CDCl_3$): δ = 7.28 (m, 4H, Ar), 7.20–7.19 (m, 2H, Ar), 7.02 (d, J = 4.0 Hz, 2H, Ar), 6.75 (m, 2H, Ar), 3.76 (t, J = 8.0 Hz, 2H, $NCH_2CH_2(CH_2)_{13}CH_3$), 3.41 (s, 2H, C≡CH), 1.78–1.75 (m, 2H, $NCH_2CH_2(CH_2)_{13}CH_3$), 1.40–1.25 (m, 26H, $NCH_2CH_2(CH_2)_{13}CH_3$), 0.90 ppm (t, J = 8.0 Hz, 3H, $NCH_2(CH_2)_{14}CH_3$). ^{13}C NMR ($CDCl_3$): δ = 145.37, 144.57, 134.45, 128.40, 125.28, 124.71, 124.69, 122.16, 120.56, 115.66 (Ar), 82.20 (C≡C), 47.88, 32.22, 30.02, 29.97, 29.94, 29.84, 29.68, 29.50, 27.12, 26.92, 23.00, 14.46 ppm ($C_{16}H_{33}$). FAB-MS: m/z = 636 (M^+). Anal. Calc. for $C_{40}H_{45}NS_3$: C, 75.54; H, 7.13; N, 2.20. Found: C, 75.38; H, 7.01; N, 2.17%.

L2: Deep yellow solid (62%). *Spectral data*: IR (KBr): 2106 cm^{-1} (C≡C), 3300 cm^{-1} (C≡CH). ^1H NMR ($CDCl_3$): δ = 7.36–7.33 (m, 4H, Ar), 7.18 (m, 2H, Ar), 7.12–7.08 (m, 4H, Ar), 7.02 (m, 2H, Ar), 6.82 (d, J = 8.0 Hz, 2H, Ar), 3.84 (t, J = 8.0 Hz, 2H, $NCH_2CH_2(CH_2)_{13}CH_3$), 3.41 (s, 2H, C≡CH), 1.83–1.79 (m, 2H, $NCH_2CH_2(CH_2)_{13}CH_3$), 1.44–1.24 (m, 26H, $NCH_2CH_2(CH_2)_{13}CH_3$), 0.88 ppm (t, J = 8.0 Hz, 3H, $NCH_2(CH_2)_{14}CH_3$). ^{13}C NMR ($CDCl_3$): δ = 144.24, 143.02, 139.25, 134.96, 134.01, 128.45, 125.31, 124.79, 124.59, 124.33, 122.99, 122.91, 120.33, 115.48 (Ar), 82.29 (C≡C), 47.66, 31.94, 29.72, 29.68, 29.64, 29.53, 29.38, 29.21, 26.85, 26.73, 22.71, 14.15 ppm ($C_{16}H_{33}$). FAB-MS: m/z = 800 (M^+). Anal. Calc. for $C_{48}H_{49}NS_5$: C, 72.04; H, 6.17; N, 1.75. Found: C, 72.12; H, 6.29; N, 1.70%.

*4.3.4. Synthesis of platinum metallopolyynes (**P0**–**P2**)*

The polymers were prepared by the dehydrohalogenative polycondensation between *trans*-[$PtCl_2(PBu_3)_2$] [110] and each of **L0**–**L2**. A typical procedure was given for **P0** starting from **L0**.

Polymerization was carried out by mixing ligand **L0** (30 mg, 0.06 mmol) and *trans*-[$PtCl_2(PBu_3)_2$] (43 mg, 0.06 mmol) in 1:1 molar ratio in NEt_3/CH_2Cl_2 (20 mL, 1:2, v/v) and CuI (3 mg) was added to the mixture as a catalyst. After stirring at room temperature for 15 h under nitrogen, the solution mixture was evaporated to dryness. The residue was redissolved in a small volume of CH_2Cl_2, and filtered through a silica column using the same eluent to remove ionic impurities and catalyst residues. After removal of the solvent, the crude product was purified by precipitation from MeOH. Subsequent washing with *n*-hexane and drying *in vacuo* gave a waxy yellow solid of **P0** (41 mg, 60%).

Spectral data: IR (KBr): 2095 cm^{-1} (C≡C). ^1H NMR ($CDCl_3$): δ = 7.24–7.21 (m, 4H, Ar), 6.88 (d, J = 8.0 Hz, 2H, Ar), 3.98 (m, 2H, $NCH_2(CH_2)_{14}CH_3$), 2.33–2.24 (m, 14H, $NCH_2CH_2(CH_2)_{13}CH_3$ + $PCH_2CH_2CH_2CH_3$), 1.81–1.49 (m, 50H, $NCH_2CH_2(CH_2)_9CH_3$ + $PCH_2CH_2CH_2CH_3$), 1.18–1.09 ppm (m, 21H, $NCH_2(CH_2)_{10}CH_3$ + $PCH_2CH_2CH_2CH_3$). ^{13}C NMR ($CDCl_3$): δ = 142.68, 129.69, 127.75, 123.97, 123.51, 114.88 (Ar), 108.05 (C≡C), 53.71, 47.74, 32.21, 29.97, 29.88, 29.65, 29.61, 27.29, 27.18, 26.64, 26.35, 24.76, 24.63, 24.53, 24.35, 24.18, 22.98, 14.41, 14.14, 8.90 ppm ($C_{16}H_{33}$ + PBu_3). ^{31}P NMR ($CDCl_3$): δ = 4.07 ppm ($^1J_{Pt-P}$ = 2357 Hz). Anal. Calc. for $(C_{56}H_{93}NP_2PtS)_n$: C, 62.89; H, 8.77; N, 1.31. Found: C, 62.76; H, 8.89; N, 1.15%. GPC (THF): M_w = 11350, M_n = 5720. PDI = 1.98.

P1: Deep yellow solid (58%). *Spectral data*: IR (KBr): 2090 cm^{-1} (C≡C). ^1H NMR ($CDCl_3$): δ = 7.27 (m, 4H, Ar), 6.97 (m, 2H, Ar), 6.77 (m, 4H, Ar), 3.82 (m, 2H, $NCH_2(CH_2)_{14}CH_3$), 2.11 (m, 14H, $NCH_2CH_2(CH_2)_{13}CH_3$ + $PCH_2CH_2CH_2CH_3$), 1.59–1.24 (m, 50H, $NCH_2CH_2(CH_2)_{13}CH_3$ + $PCH_2CH_2CH_2CH_3$), 0.95–0.87 ppm (m, 21H, $NCH_2(CH_2)_{10}CH_3$ + $PCH_2CH_2CH_2CH_3$). ^{13}C NMR ($CDCl_3$): δ = 143.89, 140.06, 129.54, 129.10, 128.85, 128.55, 124.65, 124.36, 122.00, 115.54 (Ar) 101.82 (C≡C), 47.79, 45.99, 32.16, 29.90, 29.80, 29.59, 29.49, 27.17, 26.59, 24.70, 24.63, 24.57, 24.37, 24.20, 24.03, 22.92, 14.36, 14.10, 9.10 ppm ($C_{16}H_{33}$ + PBu_3). ^{31}P NMR ($CDCl_3$, H_3PO_4): δ = 4.37 ppm ($^1J_{Pt-P}$ = 2328 Hz). Anal. Calc. for $(C_{64}H_{97}NP_2PtS_3)_n$: C, 62.31; H, 7.93; N, 1.14. Found: C, 62.23; H, 8.05; N, 1.20%. GPC (THF): M_w = 16070, M_n = 8020. PDI = 2.01.

P2: Brown-yellow solid (57%). *Spectral data*: IR (KBr): 2086 cm^{-1} (C≡C). ^1H NMR ($CDCl_3$): δ = 7.35 (m, 4H, Ar), 7.12 (m, 1H, Ar), 7.08 (m, 2H, Ar), 7.03–7.00 (m, 2H, Ar), 6.95 (m, 1H, Ar), 6.83 (m, 2H, Ar), 6.76–6.72 (m, 2H, Ar), 3.85 (m, 2H, $NCH_2(CH_2)_{14}CH_3$), 2.17–1.99 (m, 14H, $NCH_2CH_2(CH_2)_{13}CH_3$ + $PCH_2CH_2CH_2CH_3$), 1.60–1.24 (m, 50H, $NCH_2CH_2(CH_2)_{13}CH_3$ + $PCH_2CH_2CH_2CH_3$), 0.98–0.86 ppm (m, 21H, $NCH_2(CH_2)_{14}CH_3$ + $PCH_2CH_2CH_2CH_3$). ^{13}C NMR ($CDCl_3$): δ = 144.00, 141.32, 136.68, 133.97, 128.83, 128.03, 124.76, 124.59, 124.20, 123.65, 123.71, 123.09, 122.86, 115.43 (Ar), 101.48 (C≡C), 53.43, 47.65, 31.93, 30.37, 29.70, 29.54, 29.37, 29.23, 26.89, 26.78, 26.38, 26.09, 25.80, 24.48, 24.17, 24.00, 23.83, 21.84, 14.13, 13.87 ppm ($C_{16}H_{33}$ + PBu_3). ^{31}P NMR ($CDCl_3$, H_3PO_4): δ = 3.38 ppm ($^1J_{Pt-P}$ = 2330 Hz). Anal. Calc. for $(C_{72}H_{101}NP_2PtS_5)_n$: C, 61.86; H, 7.28; N, 1.00. Found: C, 61.68; H, 7.34; N, 0.93%. GPC (THF): M_w = 11590, M_n = 6890. PDI = 1.68.

*4.3.5. Synthesis of platinum model complexes (**M0**–**M2**)*

All of them were synthesized following the dehydrohalogenating coupling between *trans*-[$PtCl(Ph)(PEt_3)_2$] [111] and the corresponding diterminal alkynes. A typical procedure was given for **M0** starting from **L0**.

To a stirred mixture of ligand **L0** (30 mg, 0.06 mmol) and two molar equivalents of *trans*-[$PtPh(Cl)(PEt_3)_2$] (69 mg, 0.13 mmol) in NEt_3 (15 mL) and CH_2Cl_2 (20 mL), CuI (3 mg) was added as the catalyst. The solution was stirred at room temperature for 15 h under nitrogen, after which all volatile components were removed under vacuum. The crude product was taken up in CH_2Cl_2 and purified on preparative silica TLC plates with a CH_2Cl_2/*n*-hexane mixture (3:1, v/v) as eluent. A deep yellow band consisting of **40** was obtained as a yellow solid (57 mg, 60%).

Spectral data: IR (KBr): 2095 cm^{-1} (C≡C). ^1H NMR ($CDCl_3$): δ = 7.26–7.18 (m, 4H, Ar), 7.00–6.96 (m, 4H, Ar), 6.90–6.86 (m, 4H, Ar), 6.72 (t, J = 8.0 Hz, 4H, Ar), 6.58 (d, J = 8.0 Hz, 2H, Ar), 3.69–3.66 (m, 2H, $NCH_2(CH_2)_{14}CH_3$), 1.70–1.54 (m, 26H, $NCH_2CH_2(CH_2)_{13}CH_3$ + $PCH_2CH_2CH_3$), 1.31–1.18 (m, 26H, $NCH_2CH_2(CH_2)_{13}CH_3$), 1.12–0.93 (m, 36H, PCH_2CH_3), 0.85–0.76 ppm (m, 3H, $NCH_2CH_2(CH_2)_{13}CH_3$). ^{13}C NMR ($CDCl_3$): δ = 156.50, 142.09, 139.15, 137.17, 129.34, 127.66, 127.19, 123.31, 121.10, 114.52 (Ar), 111.87, 108.95 (C≡C), 47.38, 31.88, 29.62, 29.33, 29.28, 26.97, 26.84, 22.65, 22.58, 15.18, 15.01, 14.85, 14.09, 13.52, 13.35, 13.39, 7.98, 7.91 ppm ($NC_{16}H_{33}$ + PEt_3). ^{31}P NMR ($CDCl_3$): δ = 10.89 ppm ($^1J_{Pt-P}$ = 2642 Hz). FAB-MS: m/z = 1486 (M^+). Anal. Calc. for $C_{68}H_{109}NP_4Pt_2S$: C, 54.94; H, 7.39; N, 0.94. Found: C, 55.05; H, 7.21; N, 1.09%.

M1: Deep yellow solid (57%). *Spectral data*: IR (KBr): 2082 cm^{-1} (C≡C). ^1H NMR ($CDCl_3$): δ = 7.33–7.25 (m, 8H, Ar), 6.99–6.95 (m, 6H, Ar), 6.83–6.77 (m, 6H, Ar), 3.81 (t, J = 8.0 Hz, 2H, $NCH_2(CH_2)_{14}CH_3$), 1.77–1.72 (m, 26H, $NCH_2CH_2(CH_2)_{13}CH_3$ + PCH_2CH_3), 1.28–1.25 (m, 26H, $NCH_2CH_2(CH_2)_{13}CH_3$), 1.14–1.04 (m, 36H, PCH_2CH_3), 0.89–0.86 (m, 3H, $NCH_2CH_2(CH_2)_{13}CH_3$). ^{13}C NMR ($CDCl_3$): δ = 156.25, 143.82, 139.59, 139.32, 129.65, 129.39, 128.12, 127.57, 124.67, 124.58, 124.32, 121.99, 121.55, 115.51 (Ar), 102.58 (C≡C), 47.80, 32.17, 29.94, 29.92, 29.87, 29.81, 29.61, 29.50, 27.17, 27.04, 22.94, 15.52, 15.35, 15.17, 14.38, 8.28 ($C_{16}H_{33}$ + PEt_3). ^{31}P NMR ($CDCl_3$, H_3PO_4 as the reference): δ = 11.07 ($^1J_{Pt-P}$ = 2626 Hz). FAB-MS: m/z = 1650 (M^+). Anal. Calc. for $C_{76}H_{113}NP_4Pt_2S_3$: C, 55.29; H, 6.90; N, 0.85. Found: C, 55.09; H, 6.78; N, 1.03%.

M2: Deep yellow solid (58%). *Spectral data*: IR (KBr): 2084 cm^1 (C≡C). ^1H NMR ($CDCl_3$): δ = 7.37–7.31 (m, 8H, Ar), 7.07 (d, J = 4.0 Hz, 2H, Ar), 7.03 (d, J = 4.0 Hz, 2H, Ar), 6.99–6.94 (m, 6H, Ar), 6.82–6.80 (m, 4H, Ar), 6.76 (d, J = 4.0 Hz, 2H, Ar), 3.85–3.81 (m, 2H, $NCH_2(CH_2)_{14}CH_3$), 1.81–1.71 (m, 26H, $NCH_2CH_2(CH_2)_{13}CH_3$ + PCH_2CH_3), 1.25 (m, 26H, $NCH_2CH_2(CH_2)_{13}CH_3$), 1.14–1.02 (m, 36H, PCH_2CH_3), 0.89–0.86 ppm (m, 3H, $NCH_2CH_2(CH_2)_{13}CH_3$). ^{13}C NMR ($CDCl_3$): δ = 155.88, 143.94, 141.11, 139.06, 136.82, 133.50, 129.39, 128.84, 127.66, 127.37, 124.57, 124.53, 124.16, 123.54, 123.11, 122.84, 121.37, 115.41 (Ar), 102.24 (C≡C), 53.44, 47.63, 31.94, 29.72, 29.68, 29.65, 29.55, 29.38, 29.23, 26.89, 26.78, 22.71, 15.30, 15.13, 14.96, 14.15, 8.05, 7.95 ppm ($C_{16}H_{33}$ + PEt_3). ^{31}P NMR ($CDCl_3$): δ = 9.99 ppm ($^1J_{Pt-P}$ = 2627 Hz). FAB-MS: m/z = 1815 (M^+). Anal. Calc. for $C_{84}H_{117}NP_4Pt_2S_5$: C, 55.58; H, 6.50; N, 0.77. Found: C, 55.45; H, 6.46; N, 0.92%.

4.4. Solar cell fabrication and characterization

The device structure was ITO/poly(3,4-ethylene-dioxythiophene):poly(styrene sulfonate) (PEDOT:PSS)/polymer:PCBM blend/Al. The ITO glass substrates (10 Ω per square) were cleaned by sonication in toluene, acetone, ethanol and deionized water, dried in an oven, and then cleaned with UV ozone for 300 s. As-received PEDOT:PSS solution was passed through the 0.45 μm filter and spin-coated on patterned ITO substrates at 5000 r.p.m. for 3 min, followed by baking in N_2 at 150 °C for 15 min. The metallopolyyne:PCBM (1:4 or 1:5 by weight) active layer was prepared by spin-coating the chlorobenzene solution (20 mg/mL, for example 6 mg of metallopolyyne and 30 mg of PCBM in 1.8 mL of solvent for 1:5 blend) at 1000 r.p.m. for 2 min. The substrates were dried at room temperature in low vacuum (vacuum oven) for 1 h, and then stored in high vacuum (10^{-5}–10^{-6} Torr) overnight. Al electrode (100 nm) was evaporated through a shadow mask to define the active area of the devices (2 mm diameter circle). All the fabrication procedures (except drying, PEDOT:PSS annealing and Al deposition) and cell characterization were performed in air. Power conversion efficiency was determined from *J*–*V* curve measurement (using a Keithley 2400 sourcemeter) under white light illumination (at 100 mW cm^{-2}). For white light efficiency measurements, Oriel 66002 solar light simulator with AM1.5 filter was used. The light intensity was measured by a Molectron Power Max 500D laser power meter. For the measurement of the external quantum efficiency, different wavelengths were selected with a Oriel Cornerstone 74000 monochromator, while the photocurrent was measured with a Keithley 2400 sourcemeter. The light intensity was measured with a Newport 1830-C optical power meter equipped with a 818-UV detector probe.

Acknowledgements

This work was supported by a CERG Grant from the Hong Kong Research Grants Council (HKBU202005) and a Faculty Research Grant from the Hong Kong Baptist University (FRG/06-07/II-63). Financial support from the Strategic Research Theme, University Development Fund, and Seed Funding Grant and Outstanding Young Researcher Award (administrated by The University of Hong Kong) is also acknowledged.

Appendix A. Supplementary material

Supplementary data associated with this article including synthesis of ligand precursors, absorption spectra of **L0**–**L2** and **M0**–**M2**, PL spectra of **M0**–**M2**, absorption spectra of neat films of **P1** and **P2**, solvent dependence of PL spectra of **P1** and **P2**, dark current *J*–*V* curves of the polymer solar cells with **P1**–**P2**:PCBM (1:4 and 1:5) active layers, *J*–*V* curves of the **P1**:PCBM (1:4) device for different illumination, power dependencies for the **P1**:PCBM (1:4) cells, AFM topography images of blend films for **P1**:PCBM (1:4), **P1**:PCBM (1:5), **P2**:PCBM (1:4) and **P2**:PCBM (1:5), and detailed absorption and emission data for **L0**–**L2**. Supplementary data associated with this article can be found, in the online version, at doi:10.1016/j.jorganchem.2009.02.006.

References

[1] S.E. Shaheen, D.S. Ginley, G.E. Jabbour, MRS Bull. 30 (2005) 10.
[2] K.W.J. Barnham, M. Mazzer, B. Clive, Nat. Mater. 5 (2006) 161.
[3] N. Robertson, Angew. Chem., Int. Ed. 45 (2006) 2338.
[4] M. Grätzel, Inorg. Chem. 44 (2005) 6841.
[5] C.J. Brabec, N.S. Sariciftci, J.C. Hummelen, Adv. Funct. Mater. 11 (2001) 15.
[6] K.M. Coakley, M.D. McGehee, Chem. Mater. 16 (2004) 4533.
[7] S. Günes, H. Neugebauer, N.S. Sariciftci, Chem. Rev. 107 (2007) 1324.
[8] C. Winder, N.S. Saricftci, J. Mater. Chem. 14 (2004) 1077.
[9] B.C. Thompson, J.M.J. Frechet, Angew. Chem., Int. Ed. 47 (2008) 58. and references therein.
[10] J.Y. Kim, S.H. Kim, H.H. Lee, K. Lee, W. Ma, X. Gong, A.J. Heeger, Adv. Mater. 18 (2006) 572.
[11] M. Reyes-Reyes, K. Kim, D.J. Carroll, Appl. Phys. Lett. 87 (2005) 083506.
[12] Y. Kim, S. Cook, S.M. Tuladhar, S.A. Choulis, J. Nelson, J.R. Durrant, D.D.C. Bradley, M. Giles, I. McCulloch, C.S. Ha, M. Ree, Nat. Mater. 5 (2006) 197.
[13] G. Li, V. Shrotriya, J. Huang, Y. Yao, T. Moriarty, K. Emery, Y. Yang, Nat. Mater. 4 (2005) 864.
[14] G. Li, V. Shortriya, Y. Yao, Y.J. Yang, J. Appl. Phys. 98 (2005) 043704.
[15] Y. Kim, S.A. Choulis, J. Nelson, D.D.C. Bradley, S. Cook, J.R. Durrant, Appl. Phys. Lett. 86 (2005) 063502.
[16] R. de Bettignies, J. Leroy, M. Firon, C. Sentein, Synthetic Met. 156 (2006) 510.
[17] V.D. Mihailetchi, H. Xie, B. de Boer, L.M. Popescu, J.C. Hummelen, P.W.M. Blom, L.J.A. Koster, Appl. Phys. Lett. 89 (2006) 012107.
[18] E. von Hauff, J. Parisi, V.J. Dyakonov, J. Appl. Phys. 100 (2006) 043702.
[19] K. Kim, J. Liu, M.A.G. Namboothiry, D.L. Carroll, Appl. Phys. Lett. 90 (2007) 163511.
[20] P.D. Harvey, D. Fortin, Coord. Chem. Rev. 171 (1998) 351.
[21] W.-K. Chan, C.S. Hui, K.Y.K. Man, K.W. Cheng, H.L. Wong, N. Zhu, A.B. Djurišić, Coord. Chem. Rev. 249 (2005) 1351.
[22] C.W. Tse, K.Y.K. Man, K.W. Cheng, C.S.K. Mak, W.K. Chan, C.T. Yip, Z.T. Liu, A.B. Djurišić, Chem. Eur. J. 13 (2007) 328.
[23] F. Guo, Y.G. Kim, J.R. Reynolds, K.S. Schanze, Chem. Commun. (2006) 1887.
[24] A. Köhler, H.F. Wittmann, R.H. Friend, M.S. Khan, J. Lewis, Synthetic Met. 77 (1996) 147.
[25] A. Köhler, H.F. Wittmann, R.H. Friend, M.S. Khan, J. Lewis, Synthetic Met. 67 (1994) 245.
[26] N. Chawdhury, A. Köhler, R.H. Friend, W.-Y. Wong, J. Lewis, M. Younus, P.R. Raithby, T.C. Corcoran, M.R.A. Al-Mandhary, M.S. Khan, J. Chem. Phys. 110 (1999) 4963.
[27] N. Chawdhury, M. Younus, P.R. Raithby, J. Lewis, R.H. Friend, Opt. Mater. 9 (1998) 498.
[28] M. Younus, A. Köhler, S. Cron, N. Chawdhury, M.R.A. Al-Mandhary, M.S. Khan, J. Lewis, N.J. Long, R.H. Friend, P.R. Raithby, Angew. Chem., Int. Ed. 37 (1998) 3036.
[29] A. Köhler, M. Younus, M.R.A. Al-Mandhary, P.R. Raithby, M.S. Khan, R.H. Friend, Synthetic Met. 101 (1999) 246.
[30] W.-Y. Wong, Dalton Trans. (2007) 4495.
[31] W.-Y. Wong, X.-Z. Wang, Z. He, A.B. Djurišić, C.-T. Yip, K.-Y. Cheung, H. Wang, C.S.-K. Mak, W.-K. Chan, Nat. Mater. 6 (2007) 521.
[32] W.-Y. Wong, X.-Z. Wang, Z. He, K.-K. Chan, A.B. Djurišić, K.-Y. Cheung, C.-T. Yip, A.M.-C. Ng, Y.Y. Xi, C.S.K. Mak, W.-K. Chan, J. Am. Chem. Soc. 129 (2007) 14372.
[33] W.-Y. Wong, Macromol. Chem. Phys. 209 (2008) 14.
[34] W.-Y. Wong, X.-Z. Wang, H.-L. Zhang, K.-Y. Cheung, M.-K. Fung, A.B. Djurišić, W.-K. Chan, J. Organomet. Chem. 693 (2008) 3603.
[35] L. Li, C.-L. Ho, W.-Y. Wong, K.-Y. Cheung, M.-K. Fung, W.-T. Lam, A.B. Djurisic, W.-K. Chan, Adv. Funct. Mater. 18 (2008) 2824.
[36] X.-Z. Wang, W.-Y. Wong, K.-Y. Cheung, M.-K. Fung, A.B. Djurisic, W.-K. Chan, Dalton Trans. (2008) 5484.
[37] F. Guo, K. Ogawa, Y.-G. Kim, E.O. Danilov, F.N. Castellano, J.R. Reynolds, K.S. Schanze, Phys. Chem. Chem. Phys. 9 (2007) 2724.
[38] I. Manners, Science 294 (2001) 1664.
[39] P. Nguyen, P. Gómez-Elipe, I. Manners, Chem. Rev. 99 (1990) 1515.
[40] R.P. Kingsborough, T.M. Swager, Prog. Inorg. Chem. 48 (1999) 123.
[41] A.S. Abd-El-Aziz, Macromol. Rapid Commun. 23 (2002) 995.
[42] B.J. Holliday, T.M. Swager, Chem. Commun. (2005) 23.
[43] C.-A. Fustin, P. Guillet, U.S. Schubert, J.-F. Gohy, Adv. Mater. 19 (2007) 1665.
[44] A.S. Abd-El-Aziz, E.K. Todd, Coord. Chem. Rev. 246 (2003) 3.
[45] A.S. Abd-El-Aziz, C.E. Carraher, C.U. Pittman Jr., M. Zeldin Jr., Macromolecules Containing Metal and Metal-Like Elements, vol. 5, Wiley-Interscience, New Jersey, 2005.
[46] M.O. Wolf, J. Inorg. Organomet. Polym. Mater. 16 (2006) 189.
[47] A.S. Abd-El-Aziz, I. Manners (Eds.), Frontiers in Transition Metal-Containing Polymers, Wiley-Interscience, New Jersey, 2007.
[48] Q. Zhou, Q. Hou, L. Zheng, X. Deng, G. Yu, Y. Cao, Appl. Phys. Lett. 84 (2004) 1653.
[49] M. Svensson, F. Zhang, S.C. Veenstra, W.J.H. Verhees, J.C. Hummelen, J.M. Kroon, O. Inganäs, M.R. Anderson, Adv. Mater. 15 (2003) 988.
[50] F. Zhang, W. Mammo, L.M. Andersson, S. Admassie, M.R. Andersson, O. Inganäs, Adv. Mater. 18 (2006) 2169.
[51] D. Mühlbacher, M. Scharber, M. Morana, Z. Zhu, D. Waller, R. Gaudiana, C. Brabec, Adv. Mater. 18 (2006) 2884.
[52] M. Campoy-Quiles, T. Ferenczi, T. Agostinelli, P.G. Etchegoin, Y. Kim, T.D. Anthopoulos, P.N. Stavrinou, D.D.C. Bradley, J. Nelson, Nat. Mater. 7 (2008) 158.
[53] Y.-T. Chang, S.-L. Hsu, M.-H. Su, K.-H. Wei, Adv. Funct. Mater. 17 (2007) 3326.
[54] J.Y. Kim, K. Lee, N.E. Coates, D. Moses, T.-Q. Nguyen, M. Dante, A.J. Heeger, Science 317 (2007) 222.
[55] M. Nanjo, P.W. Cyr, K. Liu, E.H. Sargent, I. Manners, Adv. Funct. Mater. 18 (2008) 470.
[56] M. Sainsbury, in: A.R. Katritzky, C.W. Rees (Eds.), Comprehensive Heterocyclic Chemistry, vol. 3, Pergamon, Oxford, UK, 1984, p. 995.
[57] W.J. Albery, A.W. Foulds, K.J. Hall, A.R. Hillman, R.G. Edgell, A.F. Orchard, Nature 282 (1979) 793.

[58] M. Ionescu, H. Mantsch, Adv. Heterocycl. Chem. 8 (1967) 83.
[59] C. Bodea, I. Silberg, Adv. Heterocycl. Chem. 9 (1968) 321.
[60] L. Valzelli, S. Garattini, in: W.G. Clark (Ed.), Principles of Psychopharmacology, Academic Press, New York, 1970. 255.
[61] C.O. Okafor, Heterocycles 7 (1977) 391.
[62] Z. Eckstein, T. Urbanski, Adv. Heterocycl. Chem. 23 (1978) 1.
[63] J. Szabo, Chem. Heterocycl. Comp. USSR (Engl. Trans.) 15 (1979) 291.
[64] M. Sainsbury, in: M. Sainsbury (Ed.), Rodd's Chemistry of Carbon Compounds, 2nd ed., vol. 4, Elsevier, Amsterdam, 1998. 575.
[65] R. McIntyre, H. Gerischer, Ber. Bunsen Ges. Phys. Chem. 88 (1984) 963.
[66] M. Sailer, M. Nonnenmacher, T. Oeser, T.J.J. Müller, Eur. J. Org. Chem. (2006) 423.
[67] M. Sailer, A.W. Franz, T.J.J. Müller, Chem. Eur. J. 14 (2008) 2602.
[68] J. Daub, R. Engl, J. Kurzawa, S.E. Miller, S. Schneider, A. Stockmann, M.R.J. Wasielewski, Phys. Chem. A 105 (2001) 5655.
[69] P. Chen, D. Westmoreland, E. Danielson, K.S. Schanze, D. Anthon, P.E.J. Neveux, T.J. Meyer, Inorg. Chem. 26 (1987) 1116.
[70] C.S. Krämer, T.J.J. Müller, Eur. J. Org. Chem. (2003) 3534.
[71] J.E. McGarrah, Y.J. Kim, M. Hissler, R. Eisenberg, Inorg. Chem. 40 (2001) 4510.
[72] J.E. McGarrah, R. Eisenberg, Inorg. Chem. 42 (2003) 4355.
[73] T.J. Wadas, S. Chakraborty, R.J. Lachicotte, Q.M. Wang, R. Eisenberg, Inorg. Chem. 44 (2005) 2628.
[74] W.D. Bates, P. Chen, D.M. Dattelbaum, W.E. Jones Jr., T.J. Meyer, J. Phys. Chem. A 103 (1999) 5227.
[75] B.W. Pfennig, P.Y. Chen, T.J. Meyer, Inorg. Chem. 35 (1996) 2898.
[76] W.E. Jones Jr., P. Chen, T.J. Meyer, J. Am. Chem. Soc. 114 (1992) 387.
[77] A.M. Brun, A. Harriman, V. Heitz, J.P. Sauvage, J. Am. Chem. Soc. 113 (1991) 8657.
[78] A. Knorr, J. Daub, Angew. Chem., Int. Ed. Engl. 107 (1995) 2925.
[79] A. Knorr, J. Daub, Angew. Chem., Int. Ed. Engl. 34 (1995) 2664.
[80] S. Takahashi, Y. Kuroyama, K. Sonogashira, N. Hagihara, Synthesis (1980) 627.
[81] N.J. Long, C.K. Williams, Angew. Chem., Int. Ed. 42 (2003) 2586.
[82] I. Manners, Synthetic Metal-Containing Polymers, Wiley-VCH, Weinheim, 2004.
[83] W.-Y. Wong, C.-L. Ho, Coord. Chem. Rev. 250 (2006) 2627.
[84] W.-Y. Wong, J. Inorg. Organomet. Polym. Mater. 15 (2005) 197.
[85] S.J. Davies, B.F.G. Johnson, M.S. Khan, J. Lewis, J. Chem. Soc., Chem. Commun. (1991) 187.
[86] J. Lewis, M.S. Khan, B.F.G. Johnson, T.B. Marder, H.B. Fyfe, F. Wittmann, R.H. Friend, A.E. Dray, J. Organomet. Chem. 425 (1992) 165.
[87] Y. Fujikura, K. Sonogashira, N. Hagihara, Chem. Lett. (1975) 1067.
[88] K. Sonogashira, S. Takahashi, N. Hagihara, Macromolecules 10 (1977) 879.
[89] K. Sonogashira, S. Kataoka, S. Takahashi, N.J. Hagihara, J. Organomet. Chem. 160 (1978) 319.
[90] M.S. Khan, M.R.A. Al-Mandhary, M.K. Al-Suti, B. Ahrens, M.F. Mahon, L. Male, P.R. Raithby, C.E. Boothby, A. Köhler, Dalton Trans. (2003) 74.
[91] S.S. Zade, M. Bendikov, Org. Lett. 8 (2006) 5243.
[92] P. Bäuerle, Adv. Mater. 4 (1992) 102.
[93] P.M. Lahti, J. Obrzut, F.E. Karasz, Macromolecules 20 (1987) 2023.
[94] J.S. Wilson, N. Chawdhury, M.R.A. Al-Mandhary, M. Younus, M.S. Khan, P.R. Raithby, A. Köhler, R.H. Friend, J. Am. Chem. Soc. 123 (2001) 9412.
[95] M.S. Khan, M.R.A. Al-Mandhary, M.K. Al-Suti, F.R. Al-Battashi, S. Al-Saadi, B. Ahrens, J.K. Bjernemose, M.F. Mahon, P.R. Raithby, M. Younus, N. Chawdhury, A. Köhler, E.A. Marseglia, E. Tedesco, N. Feeder, S.J. Teat, Dalton Trans. (2004) 2377.
[96] J. Hou, Z. Tan, Y. Yan, Y. He, C. Yang, Y. Li, J. Am. Chem. Soc. 128 (2006) 4911.
[97] C.G. Van de Walle, J. Neugebauer, Nature (London) 423 (2003) 626.
[98] P. Garcia, J.M. Pernaut, P. Hapiot, V. Wintgens, P. Valat, F. Garnier, D. Delabouglise, J. Phys. Chem. 97 (1993) 513.
[99] I. Jestin, P. Frère, N. Mercier, E. Levillain, D. Stievenard, J. Roncali, J. Am. Chem. Soc. 120 (1998) 8150.
[100] A.F. Diaz, J. Crowley, J. Bargon, G.P. Gardini, J.B. Torrance, J. Electroanal. Chem. 121 (1981) 355.
[101] Y. Harima, D.-H. Kim, Y. Tsutitori, X. Jiang, R. Patil, Y. Ooyama, J. Ohshita, A. Kunai, Chem. Phys. Lett. 420 (2006) 387.
[102] I.F. Perepichka, D.F. Perepichka, H. Meng, F. Wudl, Adv. Mater. 17 (2005) 2281.
[103] R.D. McCullough, Adv. Mater. 10 (1998) 9316.
[104] T.-L. Stott, M.O. Wolf, Coord. Chem. Rev. 246 (2003) 89.
[105] W.-Y. Wong, G.-L. Lu, K.-F. Ng, K.-H. Choi, Z. Lin, J. Chem. Soc., Dalton Trans. (2001) 3250.
[106] L.J.A. Koster, V.D. Mihailetchi, R. Ramaker, P.W.M. Blom, Appl. Phys. Lett. 86 (2005) 123509–123511.
[107] V. Dyakonov, Appl. Phys. A 79 (2004) 21.
[108] J. Xue, S. Uchida, B.P. Rand, S.R. Forrest, Appl. Phys. Lett. 84 (2004) 3013.
[109] W.R. Dawson, M.W. Windsor, J. Phys. Chem. 72 (1968) 3251.
[110] J. Chatt, R.G. Hayter, J. Chem. Soc., Dalton Trans. (1961) 896.
[111] J. Chatt, B.L. Shaw, J. Chem. Soc. (1960) 4020.